Evaluation of Magnetic Materials for Very High Frequency Power Applications

Yehui Han*, Grace Cheung*, An Li*, Charles R. Sullivan[†] and David J. Perreault*

*Laboratory for Electromagnetic and Electronic Systems
Massachusetts Institute of Technology, Room 10–171
Cambridge, Massachusetts 02139
[†]Thayer School of Engineering at Dartmouth, Hanover, NH 03755,
http://power.thayer.dartmouth.edu chrs@dartmouth.edu

Abstract—This paper investigates the loss characteristics of several commercial rf magnetic materials for power conversion applications in the 10 MHz to 100 MHz range. A measurement method is proposed that provides a direct measurement of inductor quality factor Q_L as a function of inductor current at rf frequencies, and enables indirect calculation of core loss as a function of flux density. Possible sources of error in measurement and calculation are evaluated and addressed. The proposed method is used to identify loss characteristics of different commercial rf magnetic core materials. The loss characteristics of these materials, which have not previously been available, are illustrated and compared in tables and figures. The results of this paper are thus useful for design of magnetic components for very high frequency applications.

I. Introduction

There is a growing interest in switched-mode power electronics capable of efficient operation at very high switching frequencies (e.g., $10-100$ MHz). Power electronics operating at such frequencies include resonant inverters [1]–[10] (e.g., for heating, plasma generation, imaging, and communications) and resonant dc-dc converters [1], [3], [11]–[20] (which utilize high frequency operation to achieve small size and fast transient response.) These designs utilize magnetic components operating at high flux levels, and often under large flux swings. Moreover, it would be desirable to have improved magnetic components for rf circuits such as matching networks [21]–[25]. There is thus a need for magnetic materials and components suitable for operation under high flux swings at frequencies above 10 MHz.

Unfortunately, most magnetic materials exhibit unacceptably high losses at frequencies above a few megahertz. Moreover, the few available bulk magnetic materials which are potentially suitable for frequencies above 10 MHz are typically only characterized for small-signal drive conditions, and not under the high flux-density conditions desired for power electronics. This motivates better characterization of magnetic materials for high-frequency power conversion applications.

This paper investigates the loss characteristics of several commercial rf magnetic materials under large-signal ac flux conditions for frequencies above 10 MHz. A measurement method is proposed that provides a direct, accurate measurement of inductor quality factor Q_L as a function of ac current amplitude at rf frequencies. This method also yields an accurate means to find loss density of a core material as a function of flux density at rf frequencies. We use this technique to identify the loss characteristics of several different rf magnetic materials at frequencies up to 70 MHz.

Section II of the paper introduces a method for accurately measuring the quality factor of rf inductors under large-signal drive conditions. Section III shows how to utilize these measurements to identify core loss characteristics as a function of flux density and frequency. In Section IV, we employ these techniques to identify the loss characteristics of several commercial rf magnetic-core materials. These loss characteristics, which have not previously been available, are presented and compared in tables and figures. Finally, Section V concludes the paper.

II. Measuring the Quality Factor of RF Inductors

A. Measurement Circuit and Principles

The quality factor Q_L of a cored inductor is a function of both operating frequency and ac current (or flux) level. We utilize a measurement circuit that enables Q_L to be determined at a single specified frequency across a wide range of drive levels. Inductor quality factor is simply determined as the ratio of amplitudes of two ground-referenced voltages in a resonant circuit. A schematic of the measurement circuit is shown in Fig. 1. L, R_{cu} and R_{core} model the inductor to be evaluated: L is its inductance, R_{cu} represents its copper loss and R_{core} represents its core loss at a single frequency. R_C and C model a resonant capacitor selected to resonate with the inductor at the desired frequency. C is its capacitance and R_C represents its equivalent series resistance. The input voltage V_{in} should be a pure sinusoidal wave, and is generated by a signal generator and a rf power amplifier. The amplitude and frequency of V_{in} can be tuned by the signal generator.

To understand how this circuit enables direct measurement of inductor Q_L , consider that at the resonant frequency:

$$f_s = \frac{\omega_s}{2\pi} = \frac{1}{2\pi\sqrt{LC}} \qquad (1)$$

the ratio between the output voltage amplitude V_{out-pk} and the input voltage amplitude V_{in-pk} is:
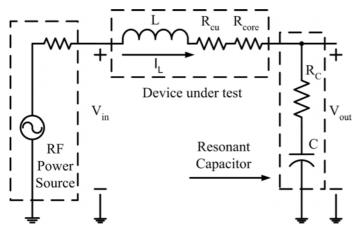
Fig. 1. Schematic of the circuit for measuring inductor quality factor, which can be calculated as the amplitude ratio V_{out-pk} over V_{in-pk}.

$$\begin{aligned} \frac{V_{out-pk}}{V_{in-pk}} &= \left| \frac{V_{out}(j\omega_s)}{V_{in}(j\omega_s)} \right| = \left| \frac{R_C + \frac{1}{j\omega_s C}}{R_{core} + R_{cu} + R_C} \right| \\ &\approx \frac{\omega_s L}{R_{core} + R_{cu}} = Q_L \end{aligned} \qquad (2)$$

The final approximation in (2) is accurate for the case in which R_C is small compared to $R_{cu} + R_{core}$ and to $\frac{1}{j\omega_s C}$, and becomes precisely true when $R_C = 0$. The above equation shows that the ratio of V_{out-pk} and V_{in-pk} is approximately equal to the quality factor of the inductor at the resonant frequency. Probing the two voltages enables direct determination of inductor Q_L. Drive level can be adjusted by varying the amplitude of the rf source. The current of the inductor is equal to the capacitor current and can be calculated from the output voltage and the known capacitor impedance. (These considerations motivate the use of high-precision low-loss capacitors such as mica or porcelain capacitors. In our experiments, we have employed microwave porcelain multi-layer capacitors from American Technical Ceramics.)

One subtlety with this measurement method is the challenge of knowing the precise resonant frequency (for which (1) and (2) apply). Given the small values of inductance that are typically of interest in the $10 - 100$ MHz range (e.g., inductances of tens to hundreds of nanoHenries [1], [2], [13]), and the correspondingly small values of resonant capacitances (tens to hundreds of picoFarads), parasitic capacitances of the measurement circuit and voltage probes can have a significant impact on the resonant frequency. Considering these influences, the resonant frequency may have up to a 5% deviation from its calculated theoretical value.

To address this issue, we pre-calculate the capacitor value to achieve the approximate resonant frequency, then adjust the frequency around the calculated resonant frequency to find the frequency point f_s' where $\frac{V_{out-pk}}{V_{in-pk}}$ has the maximum value. Let $R_L = R_{cu} + R_{core}$ represent the total source of loss in the inductor. R_C is ignored in (3), (4) and (5) as it's usually

much smaller than R_L. From (2), the derivative of $\frac{V_{out-pk}}{V_{in-pk}}$ with respect to frequency is:

$$\frac{d}{d\omega}\left(\frac{V_{out-pk}}{V_{in-pk}}\right) = -\omega C \frac{CR_L^2 + 2L(\omega^2 LC - 1)}{[\omega^2 C^2 R_L^2 + (\omega^2 LC - 1)^2]^{1.5}} \quad (3)$$

Setting $\frac{d}{d\omega}\left(\frac{V_{out-pk}}{V_{in-pk}}\right) = 0$, we find that $\frac{V_{out-pk}}{V_{in-pk}}$ reaches its maximum value at a frequency:

$$f_s' = \frac{\omega_s'}{2\pi} = \frac{1}{2\pi}\sqrt{\frac{1}{LC} - \frac{R_L^2}{2L^2}} \qquad (4)$$

From (1) and (2),

$$f_s' = f_s\sqrt{1 - \frac{1}{2Q_L^2}} \qquad (5)$$

As $Q_L \gg 1$ for all cases of interest, this frequency f_s' is approximately equal to the resonant frequency f_s. (The effect of the difference in frequency will be addressed in Section III. C.)

B. Measurement Procedures

Before beginning the measurements, an inductor is fabricated based on the frequencies and the range of flux density amplitude B_{pk} of interest. The step-by-step measurement procedures are as follows:

1) Measure the inductance: At the resonant frequency f_s, both the inductance L and the quality factor Q_L of the fabricated inductor are measured (under small-signal conditions) using an impedance analyzer. From the measured L, the resonant capacitor value can be calculated. From the measured small-signal Q_L, the expected quality factor under high-power conditions (which should be smaller than the measured small-signal Q_L) can be estimated. Though the measurement is under very low drive conditions, the core loss can't be ignored for some materials, so this small-signal Q_L measurement may reflect both core and copper loss.

2) Calculate the relative permeability μ_r: Though most core companies will specify the relative permeability μ_r of the material, μ_r should be measured and calculated to get an accurate value. Assuming that the inductor core is toroidal, from [26] we get:

$$\mu_r \approx \frac{2\pi L}{N^2 h \mu_0 \ln\left(\frac{d_o}{d_i}\right)} \qquad (6)$$

where L is the inductance measured in step 1), h, d_o and d_i are the height, the outer diameter and the inner diameter of the inductor, and N is the number of turns of the inductor. To minimize the error caused by the inductance of a single turn loop [26], N should be as large as possible. (In our experiments, we often fabricate and measure another inductor with the same core but a high turns number (> 20) specifically to reduce the single turn inductance error and get an accurate value of μ_r.)

4271

3) Select resonant capacitor: The resonant capacitor value C can be calculated from (1). C should be much larger than the potential parasitic capacitance and the probe capacitance. The precise value C and ESR R_C of the capacitor is also measured using an impedance analyzer. Q_C can be calculated from C and R_C. We assume Q_C is constant during all the measurements. When Q_C is 1000 or higher, it may be difficult to accurately measure its value. In this case, Q_C may be estimated based on data sheet values. Q_C should be ten times larger than Q_L to minimize its influence on the Q_L measurement and the loss extraction.

4) Fabricate the resonant circuit: The printed circuit board should be designed carefully to minimize parasitic inductance and capacitance. A transformer or a low pass filter of the drive input may be needed to reduce the distortion of the input voltage V_{in}.

5) Calculate the required V_{out}: The inductor current amplitude I_{L-pk} can be calculated from B_{pk} and the inductor's parameters. For example, the I_{L-pk} of a toroidal inductor can be calculated as:

$$I_{L-pk} = \frac{\pi(d_o + d_i)B_{pk}}{2\mu_r\mu_0 N} \qquad (7)$$

where B_{pk} is the flux density amplitude in the toroidal core. I_{L-pk} is also the current amplitude of the resonant capacitor. The output voltage amplitude V_{out-pk} can be calculated from I_{L-pk} and the impedance of the resonant capacitor:

$$V_{out-pk} = \frac{I_{L-pk}}{2\pi f_s C} = \frac{(d_o + d_i)B_{pk}}{4 f_s C \mu_r \mu_0 N} \qquad (8)$$

6) Set up the experiment: The experimental setup comprises a signal generator, a rf power amplifier, and an oscilloscope in addition to the fabricated resonant circuit. The signal generator drives the power amplifier to produce a sinusoidal voltage with a variable amplitude and a tunable frequency. In our system we employ an Agilent 33250A signal generator and an AR 150A100B rf power amplifier. The output of the amplifier is connected to the input of the resonant circuit by a matched cable, with any impedance transformation and/or filtering applied at the resonant circuit input. In our system, we typically employ an AVTECH AVX-M4 transmission line transformer (50 : 3 impedance transformation ratio) to better match the 50 Ω power amplifier to the low-impedance resonant circuit. We also often incorporate a low pass filter (RC) to reduce the voltage distortion at the resonant circuit input.

Note that the capacitance of the probe that measures the output voltage should be as small as possible, as it adds to the resonant capacitor value. The capacitance of the probe to measure the input voltage doesn't influence the measurement results.

7) Measure a set of V_{in-pk} and V_{out-pk}: The signal frequency is initially set to the calculated value of the resonant frequency f_s. However, due to parasitics, probe capacitance and component errors, this frequency is not exactly equal to the resonant frequency f_s. While adjusting the circuit to maintain the designed V_{out-pk} according to (8), tune the input signal

frequency finely and search for the minimum V_{in-pk}. The frequency where V_{in} reaches its minimum is f_s' which is close to f_s when Q_L is high.

Because the resonant circuit is highly tuned, the output voltage will be a very good sinusoidal waveform. However, because both the input power and input voltage V_{in} are small, the power amplifier may work in a nonlinear region and a distorted V_{in} may be observed. In this case, a transformer or a low pass filter at the resonant circuit input can help to reduce the distortion. If the distortion can't be ignored, the magnitude of V_{in} at f_s' can be calculated numerically by Fourier analysis.

Using the tuning characteristics, we can also determine if μ_r varies significantly with current level. If μ_r changes, the inductance will change and the tuned resonant frequency f_s' will also change. If this happens, the inductance L and the relative permeability μ_r need to be recalculated based on the resonant capacitor value C and the tuned f_s'. Knowing V_{in-pk} and V_{out-pk}, Q_L can be calculated from (2).

Fig. 2 shows a representative curve of Q_L vs. current drive level at 30 MHz for a 190 nH inductor wound with 5 turns of foil on an M3 ferrite core. The strong variation of Q_L with ac current level (owing to core loss) is readily observed.
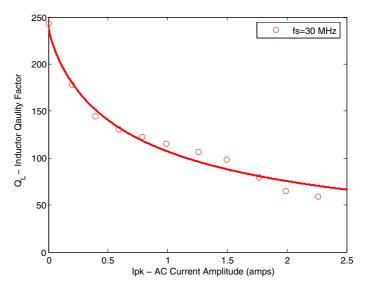

Fig. 2. The Q_L of fabricated inductor with an M3 toroidal core (OD= 12.7 mm, ID= 7.82 mm, Ht= 6.35 mm) with $N = 5$ turns, and $L = 190$ nH.

III. Extraction of Loss Characteristics of Commercial RF Magnetic Cores

In this section we show how the quality factor measurements of Section II can be adapted to identify core loss characteristics of magnetic materials. We do not seek to identify or model the underlying cause of core losses [27], [28]. Rather, we focus on quantitatively identifying the power loss density of a given magnetic material as a function of flux density under sinusoidal excitation at a specified frequency. Numerous works illustrate how this information can be used in the design of magnetic components, even for systems with complex excitations [29]–[31].

Methods and guidelines exist for direct measurement of core loss through voltage and current measurements made on multi-winding structures [32]–[34]. However, these methods rely on very accurate measurement of phase relationships between voltages and currents, which becomes increasingly hard to do as frequency increases. Instead, we exploit an indirect method: Starting with an accurate measurement of total inductor loss (from accurate measurement of inductor Q_L), we seek to extract the portion of loss owing to the magnetic core. In the subsections that follow, we describe preparations and measurements of single-layer, foil-wound toroids (of materials to be tested), from which core loss information can be extracted.

A. Design and Fabrication of Low-loss Inductors with Toroidal Cores

To identify the loss characteristics of a magnetic-core material, the quality factor of inductors fabricated with appropriate magnetic cores are measured under large-signal drive conditions. We focus on ungapped toroidal magnetic cores due to the availability of these cores, the simplicity and uniformity of the calculations, and the magnetic self shielding provided by this core type.

The fabricated inductor should have as small a copper loss as possible compared to its core loss in order to minimize error. For this reason, we utilize a single-layer copper foil winding on the toroidal core. (Even more sophisticated construction techniques are possible [26], but are not used here.)

The copper foil is cut in the shape of a narrow strip. The following equations show the parameters of the copper strip and fabricated inductor.

$$N \approx \sqrt{\frac{2\pi L}{h\mu_r\mu_0 \ln\left(\frac{d_o}{d_i}\right)}} \tag{9}$$

where N is the number of turns, L is the inductance, μ_r is the relative permeability of the magnetic material, μ_0 is the permeability of free space, and h, d_i and d_o are the height, inner diameter and outer diameter of the toroidal core. Note that the thickness t_{cu} of the foil should be larger than a skin depth in order to get the minimum resistance:

$$t_{cu} > \delta = \sqrt{\frac{\rho_{cu}}{\pi\mu_0 f_s}} \tag{10}$$

where ρ_{cu} is the electrical conductivity of copper.

The width of the copper foil is selected as:

$$w_{cu} \approx \frac{\pi d_i}{N} \tag{11}$$

to achieve the desired number of turns. In fabrication, a value of w_{cu} is a little smaller than the above value is employed to leave a space between the turns of the foil winding.

The foil winding length is approximately:

$$l_{cu} = N(2h + d_o - d_i) \tag{12}$$

where the length l_{cu} of foil does not include the length of extra copper terminals to be soldered on the PCB pad. Because

the relative permeability μ_r of the magnetic core is high ($>$ 4) and the toroidal inductor is self-shielded, we assume that most of the flux is inside the core. Fig. 3 shows an inductor fabricated by the above method. The core is M3-998 from National Magnetics Group.

Fig. 3. An example of an inductor fabricated from copper foil and a commercial magnetic core.

B. The Extraction of Core Loss Characteristics from the Measurement Results.

The core loss characteristics can be extracted from the measured value of Q_L (based on V_{in-pk}, V_{out-pk} and f'_s). The measured quality factor Q_L provides a measure of the total loss. By subtracting out an estimate of the copper loss, we are left with an estimate of the core loss (and core loss density).

Referring to Fig. 1, we have:

$$Q_L \approx \frac{V_{out-pk}}{V_{in-pk}} = \frac{2\pi f_s L}{R_{core} + R_{cu} + R_C} \tag{13}$$

and

$$R_{core} = \frac{2\pi f_s L V_{in-pk}}{V_{out-pk}} - R_C - R_{cu} \tag{14}$$

The resistance of the resonant capacitor R_C can be measured by an impedance analyzer or acquired through the data sheet. It is more difficult to establish R_{cu}'s exact value. We employ the following method estimate the value for R_{cu}. We fabricate an air-core inductor with the same dimension and measure its R_{cu} using an impedance analyzer. From finite element simulation results, this value is close to the R_{cu} of a cored inductor for $\mu_r < 4$. When $\mu_r \geq 4$, this value can be lower than the R_{cu} of a cored inductor by up to 30%. So we consider that this estimation of R_{cu} has up to 30% error. In our experiments, the core loss is controlled to be at least 5 times larger than the copper loss to reduce the error caused by R_{cu}.

With a value for R_{core}, the average core loss can be calculated. We express our results as core loss per unit volume as a function of flux density.

$$P_V = \frac{I_{L-pk}^2 R_{core}}{2V_L} \tag{15}$$

where V_L is the volume of the core. Because B_{pk} is specified, one data point of B_{pk} versus P_V (mW/cm^3) is acquired.

C. The Estimation of Errors

Possible errors in this procedure are discussed below:

1) Error caused by the capacitor ESR: As indicated in (2), capacitor ESR influences the voltage ratio, making it deviate from the desired Q_L value. The error due to R_C can be estimated. For example, if $Q_L = 100$ and $Q_C > 1000$, then $R_C < 10\% R_L$ and the denominator of (2) has less than 10% error. If we estimate Q_C as about 2000, the error in Q_L caused by R_C will be approximately 5%.

2) Error caused by circuit parasitics: As described preciously, the values of the resonant capacitor and the inductor are controlled to be much larger than the circuit parasitic capacitance or inductance to minimize their influence on the resonant frequency f_s. However, the parasitics can have a very poor Q, (i.e., relatively a high series ac resistance and low parallel ac resistance) which add extra losses. The error can be further reduced by a careful layout. The pads of the resonant inductor should be as close as possible to the pads of the resonant capacitor and the measurement points to reduce the trace inductance and resistance. The resonant capacitor should be also connected to the ground tightly to reduce parasitic series resistance and inductance. With sufficient effort, error due to these parasitics can be made negligibly small and is not considered further in this paper.

3) The error caused by copper loss: The error caused by the copper loss (represented by resistance R_{cu}) can be a severe problem if $R_{core} \leq R_{cu}$. An exact value for the winding resistance R_{cu} is hard to determine. However, if $R_{core} \gg R_{cu}$, the error introduced by inaccuracies in the estimated value of R_{cu} is small. For example, if $R_{core} \geq 5R_{cu}$ and an error of up to 30% in the estimate of R_{cu} occurs, the R_{core} error caused by R_{cu} will be less than 5%.

4) Error caused by the resonant frequency f_s': Though the difference between f_s' and f_s is small when Q_L is high, the error should be analyzed carefully. Assume the error of the frequency is 1%. While V_{out-pk} is constant, the error of the inductor's current is about 1% and the error of the flux density in the inductor core is 1%. If $P_V \propto f_s^\xi B_{pk}^\beta$, and both ξ and β are about 2.6 to 2.8, the error of P_V will be less than 5.6%. However, the error can be compensated for by knowing f_s' and the approximate value of Q_L.

5) Error caused by uneven flux density: The flux density in a toroidal core is not even, which means the inner part of the core has more power loss than the outer part. This error depends on the dimensions of the core, mainly determined by the ratio of d_o and d_i. For $d_o = 2d_i$ and $\beta = 2.8$., the error is about 10%. However, the error can be also compensated (see [32], for example).

6) The total error: Considering all these error factors, the total error will be less than 20% if the inductor and the circuit are well designed and fabricated, $R_{core} \gg R_{cu}$, and the measurement is done carefully.

IV. CORE LOSS MEASUREMENTS IN COMMERCIAL MAGNETIC MATERIALS

Here we apply the proposed methods to identify the large-signal loss characteristics of several commercial rf magnetic materials. The loss characteristics of these materials under large flux-swing condition have not been previously available, and are expected to be useful for design of rf power magnetic components. Table I shows the magnetic materials for which data will be provided. The loss characteristics of the materials listed in Table I are plotted in Figs. 4–8. At 20 MHz, the core loss of -17 material is too small to be measured and extracted. Moreover, it has a useful range extending to higher frequencies. Thus we measured it in a somewhat different range. In Fig. 4 to 8, the Steinmetz equation $P_V = KB_{pk}^\beta$ is used to fit the data. Table II shows K and β for each of these materials.

TABLE I
MATERIALS, SUPPLIERS AND SPECIFICATIONS

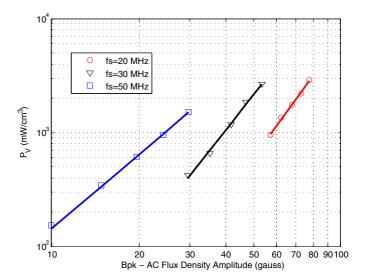| Material	Type	Supplier	Permeability
M3	NiZn	National Magnetics Group	12
P	CoNiZn	Ferronics	40
67	NiZn	Fair-rite	40
N40	NiZn	Ceramic Magnetics	15
-17	Powered iron	Micrometals	4

Fig. 4.   M3 Material Core Loss vs AC Flux Density.

V. CONCLUSION

In this paper, the authors investigate the loss characteristics of several commercial rf magnetic materials for power conversion applications at very high frequencies (10 MHz to 100 MHz). A experimental method is proposed to directly measure inductor quality factor. The loss characteristics of these materials are further extracted based on the quality factor measurements. It is hoped that the presented data and methods will be of value in the design of magnetic components for very high frequency applications.

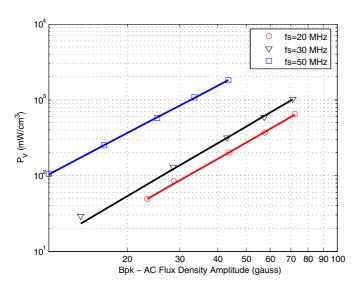| Material	20 MHz		30 MHz		50 MHz		70 MHz	
	K	β	K	β	K	β	K	β
M3	8.28×10^{-4}	3.46	6.75×10^{-3}	3.24	1.03	2.15	—	—
P	3.57×10^{-2}	2.29	5.06×10^{-2}	2.33	6.96×10^{1}	2.09	—	—
67	1.42×10^{-1}	2.12	2.10×10^{-1}	2.18	1.15	2.05	—	—
N40	3.64×10^{-2}	2.23	2.27×10^{-1}	2.02	2.08×10^{-1}	2.58	—	—
-17	—	—	3.61×10^{-2}	2.76	1.86	2.10	2.35	2.22

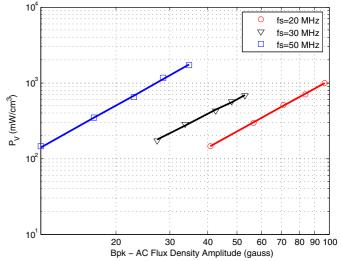Fig. 5.   P Material Core Loss vs AC Flux Density.

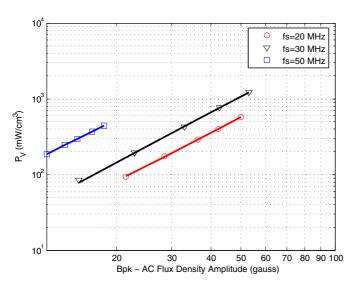Fig. 7.   N40 Material Core Loss vs AC Flux Density.

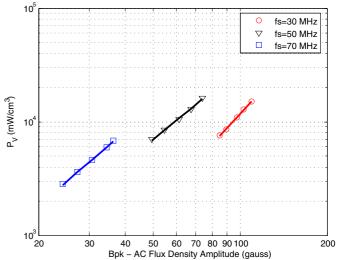Fig. 6.   67 Material Core Loss vs AC Flux Density.

Fig. 8.   -17 Material Core Loss vs AC Flux Density. Note that because the permeability of this material is low ($\mu_r = 4$), it is difficult to separate core loss from copper loss. Consequently, the core was operated at extremely high loss densities under forced convection cooling in order to facilitate separation of core loss from copper loss. In many practical designs, one might choose to operate at lower loss densities than utilized here.

REFERENCES

[1] J. Rivas, "Radio frequency dc-dc power conversion," Ph.D. dissertation, Massachusetts Institute of Technology, Sep. 2006.

[2] J. M. Rivas, Y. Han, O. Leitermann, A. Sagneri, and D. J. Perreault, "A high-frequency resonant inverter topology with low voltage stress," *38th IEEE Power Electronics Specialists Conf.*, pp. 2705–2717, Jun. 2007.

[3] D. C. Hamill, "Class DE inverters and rectifiers for DC-DC conversion," in *27th IEEE Power Electronics Specialists Conf.*, vol. 1, Baveno, Jun. 1996, pp. 854–860.

[4] N. O. Sokal and A. D. Sokal, "Class E-a new class of high-efficiency tuned single-ended switching power amplifiers," *IEEE J. Solid-State Circuits*, vol. 10, no. 3, pp. 168–176, Jun. 1975.

[5] N. O. Sokal, "Class-E rf power amplifiers," *QEX*, pp. 9–20, Jan./Feb. 2001.

[6] R. Frey, "High voltage, high efficiency mosfet rf amplifiers - design procedure and examples," Advanced Power Technology, Application Note APT0001.

[7] ——, "A push-pull 300-watt amplifier for 81.36 MHz," Advanced Power Technology, Application Note APT9801, 1998.

[8] ——, "500w, class e 27.12 MHz amplifier using a single plastic mosfet," Advanced Power Technology, Application Note APT9903, Jun. 1999.

[9] M. Iwadare and S. Mori, "Even harmonic resonant class E tuned power amplifer without rf choke," *Electron. and Commun. in Japan I, Commun.*, vol. 79, no. 12, pp. 23–30, Jan. 1996.

[10] S. D. Kee, I. Aoki, A. Hajimiri, and D. Rutledge, "The class-E/F family of ZVS switching amplifiers," *IEEE Trans. Microw. Theory Tech.*, vol. 51, no. 6, pp. 1677–1690, Jun. 2003.

[11] A. Sagneri, "Design of a very high frequency dc-dc boost converter," Master's thesis, Massachusetts Institute of Technology, Feb. 2007.

[12] W. C. Bowman, F. T. Balicki, F. T. Dickens, R. M. Honeycutt, W. A. Nitz, W. Strauss, W. B. Suiter, and N. G. Ziesse, "A resonant dc-to-dc converter operating at 22 megahertz," in *3rd Annu. IEEE Applied Power Electronics Conf. and Expo.*, New Orleans, LA, Feb. 1988, pp. 3–11.

[13] R. Pilawa-Podgurski, A. Sagneri, J. M. Rivas, D. Anderson, and D. J. Perreault, "Very high frequency resonant boost converters," *38th IEEE Power Electronics Specialists Conf.*, pp. 2718–2724, Jun. 2007.

[14] R. J. Gutmann, "Application of RF circuit design principles to distributed power converters," *IEEE Trans. Ind. Electron. Contr. Instrum.*, vol. 27, no. 3, pp. 156–164, Aug. 1980.

[15] J. J. Jóźwik and M. K. Kazimierczuk, "Analysis and design of class-E^2 DC/DC converter," *IEEE Trans. Ind. Electron.*, vol. 37, no. 2, pp. 173–183, Apr. 1990.

[16] S. Ajram and G. Salmer, "Ultrahigh frequency DC-to-DC converters using GaAs power switches," *IEEE Trans. Power Electron.*, vol. 16, no. 5, pp. 594–602, Sep. 2001.

[17] R. L. Steigerwald, "A comparison of half-bridge resonant converter topologies," *IEEE Trans. Power Electron.*, vol. 3, no. 2, pp. 174–182, Apr. 1988.

[18] R. Redl and N. O. Sokal, "A 14-MHz 100-watt class E resonant converter: Principle, design considerations and measured performance," in *17th IEEE Power Electronics Specialists Conf.*, 1986, pp. 68–77.

[19] W. A. Tabisz and F. C. Lee, "Zero-voltage-switching multi-resonant technique-a novel approach to improve performance of high frequency quasi-resonant converters," in *19th IEEE Power Electronics Specialists Conf.*, Kyoto, Japan, Japan, Apr. 1988, pp. 9–17.

[20] F. C. Lee, "High-frequency quasi-resonant converter technologies," *Proceedings of the IEEE*, vol. 76, no. 4, pp. 377–390, Apr. 1988.

[21] Y. Han and D. J. Perreault, "Analysis and design of high efficiency matching networks," *IEEE Trans. Power Electron.*, vol. 21, no. 5, pp. 1484–1491, Sep. 2006.

[22] C. Bowick, *RF Circuit Design*. London, UK: Newnes, 1997, ch. 3.

[23] W. L. Everitt and G. E. Anner, *Communication Engineering*, 3rd ed. McGraw-Hill Book Company, 1956, ch. 11.

[24] T. Lee, *The Design of CMOS Radio-Frequency Integrated Circuits*, 2nd ed. Cambridge, UK: Cambridge University Press, 2004, pp. 87–107.

[25] E. Gilbert, "Impedance matching with lossy components," *IEEE Trans. Circuits Syst.*, vol. 22, no. 2, pp. 96–100, Feb. 1975.

[26] C. R. Sullivan, W. Li, S. Prabhakara, and S. Lu, "Design and fabrication of low-loss toroidal air-core inductors," *38th IEEE Power Electronics Specialists Conf.*, pp. 1757–1759, Jun. 2007.

[27] G. Bertotti, "General properties of power losses in soft ferromagnetic materials," *IEEE Trans. Magn.*, vol. 24, no. 1, pp. 621–630, Jan. 1988.

[28] J. Goodenough, "Summary of losses in magnetic materials," *IEEE Trans. Magn.*, vol. 38, no. 5, pp. 3398–3408, Sep. 2002.

[29] W. A. Roshen, "A practical, accurate and very general core loss model for nonsinusoidal waveforms," *IEEE Trans. Power Electron.*, vol. 22, no. 1, pp. 30–40, Jan. 2007.

[30] J. Li, T. Abdallah, and C. R. Sullivan, "Improved calculation of core loss with nonsinusoidal waveforms," in *36th Annual Meeting of IEEE Industry Applications Society*, vol. 4, Chicago, IL, Sep./Oct. 2001, pp. 2203–2210.

[31] K. Venkatachalam, C. R. Sullivan, T. Abdallah, and H. Tacca, "Accurate prediction of ferrite core loss with nonsinusoidal waveforms using only steinmetz parameters," in *2002 IEEE Workshop on Computers in Power Electronics*, Jun. 2002, pp. 36–41.

[32] A. F. Goldberg, "Development of magnetic components for 1-10 MHz dc/dc converters," Ph.D. dissertation, Massachusetts Institute of Technology, Sep. 1988.

[33] "IEEE standard for test procedures for magnetic cores," IEEE Standard 393-1991, March 1992.

[34] "Cores made of soft magnetic materials–measuring methods," IEC International Standard 62044-1, 2002-2005.